1316

NASA TECHNICAL MEMORANDUM

NASA TM-88387

ANISOTROPY OF HIGH TEMPERATURE STRENGTH IN PRECIPITATION-HARDENED NICKEL-BASE SUPERALLOY SINGLE CRYSTALS

Y.G. Nakagawa, H. Terashima, H. Yoshizawa,
Y. Ohta, and K. Murakami

Translation of "Sesshutsu koka-kei Ni kichō gōkin tankesshō no ihōsei", Ishikawajima-Harima Engineering Review (ISSN 0578-7904), Vol. 25, Jan. 1985, p. 5-10.

NATIONAL AERONAUTICS AND SPACE ADMINISTRATION
WASHINGTON, D.C. 20546 MARCH 1986

STANDARD TITLE PAGE

1. Report No. NASA TM-88387	2. Government Accession No.	3. Recipient's Catalog No.
4. Title and Subtitle ANISOTROPY OF HIGH TEMPERATURE STRENGTH IN PRECIPITATION-HARDENED NICKEL-BASE SUPERALLOY SINGLE CRYSTALS		5. Report Date March 1986 6. Performing Organization Code
7. Author(s) Y. Nakagawa, H. Terashima, H. Yoshizawa, Y. Ohta, and K. Murakami (Technical Headquarters of the Technological Research Laboratory, Metal Materials Dept.)		8. Performing Organization Report No. 10. Work Unit No.
9. Performing Organization Name and Address Leo Kanner Associates Redwood City, California 94063		11. Contract or Grant No. NASW-4005 13. Type of Report and Period Covered Translation
12. Sponsoring Agency Name and Address National Aeronautics and Space Administration Washington, D.C. 20546		14. Sponsoring Agency Code

15. Supplementary Notes

Translation of "Sesshutsu koka-kei Ni kichō gōkin tankesshō no ihōsei", Ishikawajima-Harima Engineering Review (ISSN 0578-7904), Vol. 25, Jan. 1985, p. 5-10.

(A85-38443)

16. Abstract

Anisotropy of high temperature strength of nickel-base superalloy, Alloy 454, being in service for advanced jet engine turbine blades and vanes, was investigated by us. Crystallographic orientation dependence of tensile yield strength, creep and creep rupture strength was found to be marked at about 760°C. In comparison with other single crystal data, a larger allowance in high strength off-axial orientation from the 001 axis, and relatively poor strength at near the -111 axis were noted. From transmission electron microscopy the anisotropic characteristics of this alloy were explained in terms of available slip systems and stacking geometries of gamma-prime precipitate cuboids which are well hardened by large tantalum content. §100† cube slip was considered to be primarily responsible for the poor strength of the -111 axis orientation replacing the conventional §111† plane slip system.

(Author)

17. Key Words (Selected by Author(s))	18. Distribution Statement Unclassified-Unlimited		
19. Security Classif. (of this report) Unclassified	20. Security Classif. (of this page) Unclassified	21. No. of Pages 25	22.

ANISOTROPY OF HIGH TEMPERATURE STRENGTH IN PRECIPITATION-HARDENED NICKEL-BASE SUPERALLOY SINGLE CRYSTALS

Y.G. Nakagawa, H. Terashima, H. Yoshizawa,
Y. Ohta, and K. Murakami
Technical Headquarters of the
Technological Research Laboratory,
Metal Materials Dept.

1. Introduction

/5*

There is a recent trend for the use of nickel-based superalloy precision cast parts made entirely with a single molecular alignment in high-pressure turbine vanes of jet engines, with its use expanding to an increasing number of engine makers. These single crystalline vanes do not require structural elements such as C, B, Zr, Hf, etc. which were used to reinforce the crystal grain boundaries, a weakness of past alloys, remarkably increasing the amount of freedom in alloy design [1]. These grain boundary accumulating elements tended to lower the local melting temperature of the product, which limited its post-casting solution treatment temperature to below its partial melting temperature, since this problem does not exist with single crystals, solution treatment temperatures can be greatly increased, making possible the more uniform dispersion of elemental- or precipitation-hardeners (gamma'). Another characteristic of single crystals is the fact that vane performance can be optimized by making the crystal alignment an important element in the vane design. Ni-based superalloys are

* Numbers in the margin indicate pagination of the foreign text.

entirely constructed of a face-centered cubic lattice (fcc), making them rich in geometric crystal symmetry, but, in contrast to the fact that most conventional polycrystalline vanes are isotropic by nature of their texture of various crystal alignments, single crystalline vanes possess a strong anisotropy in the relationship between the vane axis and the crystal orientation [2][3][4]. The elastic constant, tensile strength, creep and creep rupture strengths and low cycle fatigue, etc. are considered anisotropies which are essential in the design of turbine vanes, but we are presently still at the stage of advancing our clear understanding of these [5][6].

This article is a report of the results of studies of the high temperature tensile strength and creep strength of Alloy 454 [1], an alloy which exclusively uses single crystals. There are several places in this article where an intimate knowledge of the components used in PWA JT 9 D-7 R 4 and T 400-WV-402 moving and static vanes and their properties may be required. We understand that this testing reveals some elements which may differ from the generally accepted data on the anisotropy of the high temperature strength of single crystals [4][5], but we have come to these conclusions from the results of the observation of dislocated structures through transparent electron microscopy (TEM).

2. Methodology

The standard compositions of the reference alloys, Mar-M 200 and Mar-M 247, whose data will be used for comparison with the Alloy 454 used in this testing, are shown in Table 1. These are

composed with a tantalum, molybdenum or tungsten-reinforced gamma' phase $Ni_3(Al,Ti)$, which is based on the fcc structure of an $L1_2$ standard phase, dispersed in a Ni solid solution (fcc, gamma phase), which has been precipitation reinforced with cobalt, chromium, molybdenum or tungsten. A single crystal

Table 1

Chemical composition of Alloy 454 and standard composition of reference alloys

item / sample	Chemical Content (%)												notes
	Cr	Co	Mo	W	Ti	Al	Ta	C	B	Zr	Ni	other	
Alloy 454	9.85	4.9	--	3.95	1.6	5.05	11.85	--	--	--	bal.	--	exclusively SC alloy
Mar-M 200	9.0	10.0	--	12.5	2.0	5.0	--	0.15	0.015	--	bal.	1 Nb	reference alloy
Mar-M 247	8.4	10.0	0.6	10.0	1.0	5.5	3.0	0.15	0.015	0.05	bal.	--	reference alloy

casting, close in form to the final product, was manufactured in an existing directional solidification (DS) furnace, at a pouring temperature of 1550°C, a casting heating furnace temperature of 1530°C and a pull-down rate of 200 mm/hour, using an ingot of Alloy 454. The parallel components of this test sample were ϕ6 x 30 mm in dimension, and possessed a rim extending from each end of the parallel components for detection. After 4 hours of solution treatment at 1280°C, the test sample was cooled and then immediately aged for 32 hours at 871°C [1]. The orientation of the tensile axis were determined by determining the orientation of the edges of the test sample using Laue's reverse X-ray method. Tensile testing consisted of performing temperature dependency testing at RT, 700, 760, 800, 900 and 1000°C and performing orientation dependency testing at 760°C and 900°C.

Creep testing consisted of performing temperature dependency testing at 760, 800, 900, 982 and 1000°C and performing orientation dependency testing under conditions of 77.3 kgf/mm_2 at 760°C (760 MPa) and 20.5 kgf/mm_2 at 982°C (200 MPa). In the temperature dependency testing of both sets of tests, tensile axes of within 10° off-axis from the 001 axis were used as samples. The distribution of the tensile axis orientations of the samples used in orientation dependency testing will be shown in the following. After testing, samples of representative orientations were sliced from each parallel component of the test sample, made into thin films by twin-jet electrolytic polishing and observed through H 700 TEM for dislocation structure.

3. Results

/6

3.1 Temperature Dependency

The vane axis of turbine vanes presently in service is near the 001 axis, while the samples used for this temperature dependency testing were also selected from those with a tensile axis of within 10° off-axis from the 001 axis and evaluated. To conserve space in this article, we will not go into extreme detail, but according to the tensile strength testing, this alloy showed a 0.2% durability (σ_y) and tensile strength (σ_B), as well as temperature dependency, equal to or greater than that listed in available data on cubic and columnar Mar-M 247. These values increase gradually until 700 to 800°C, and decrease in excess of that. Fracture creep (σ) displayed behavior of nearly the same level, showing extremely low values in the region between 700 and

800°C. The gamma' phase volumetric content of both Alloy 454 and Mar-M 247 was near 60%, but the gamma' phase in these alloys differed from that of common alloys wherein it displayed increased strength accompanying increases in temperature, showing a close relationship between the high temperature properties of these alloys and the peculiarity of their gamma' phases. The results of the temperature dependency of creep rupture strength are shown in Figure 1, plotted using the Larson-Miller parameter, showing strength greater than that shown in data on the reference alloys and correlating well with documented values [7] for this alloy.

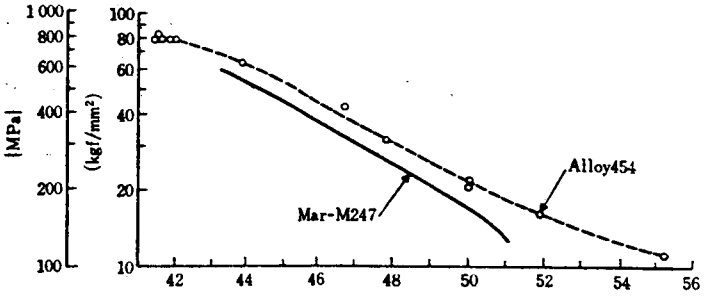

Larson-Miller parameter, $1.8T(20 + \log t) \times 10^{-3}$

(notes) ϕ6 mm
solution treatment: 1285°C x 4h
aging : 871°C x 32h
tensile axis is within 10° off-axis from the 001 axis

Fig. 1 Larson-Miller plotting of creep rupture strength

3.2 Crystal Orientation Dependency

Evaluation of the dependency of tensile strength on crystal orientation was performed using the 760°C and 900°C σ_y results and the 760°C and 982°C results of creep testing. Before

testing, tensile axis orientations from an angle from the 001 axis to the 011 axis were plotted in standard sterographic triangles [8] and the strength data shown as coefficients placed near the tensile axis plots. Figures 2-(a)(b) show the distribution of various σ_y at 760°C and 900°C. At 760°C, σ_y at orientations near the -111 to 011 axis boundary are low, with anisotropy of up to approximately 3/4 of those near the 001 axis, while, at 900°C, data figures are scarce, but from other information, it is conjectured that anisotropy is low. Figures 3-(a) through (c) show the rupture life, rupture creep and minimum creep results, respectively, of creep strength testing at 760°C under 77.3 kgf/mm$_2$ (760 MPa), while Figures 3-(a') through (c') similarly show these results at 982°C under 20.5 kgf/mm$_2$ (200 MPa). Similar to o_y, marked anisotropy was displayed at 760°C, while the data at the higher temperature is also at nearly the same level. In contrast to existing anisotropy data, which shows decreased creep strength

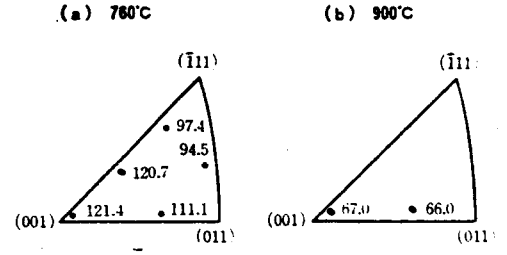

Fig. 2 Stereographic triangles showing yield strength

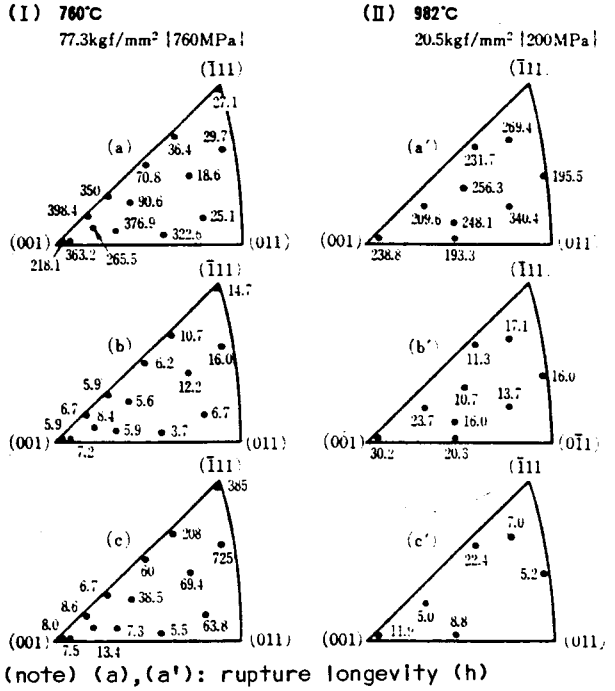

Fig. 3 Stereographic triangle presentation of creep test results

and longevity when there is a greater than 10° slip from the 001 axis, while is veritably no change in this alloy within even 20°off-axis from 001. Compared to other alloys, there is a remarkable difference in tensile axes, particularly above the 001 to -111 boundary.

A secondary characteristic is that, in comparison to other alloys which possess good tensile strength in this are, samples near the -111 axis (H22) showed extremely low strength in this alloy, it being nearly equal to the strength near the 001 axis (which is also a minimal strength orientation in the reference alloys).

The tensile axis orientation of the samples used for metallography in this testing are shown in Figure 4. TEM metallography was performed mainly on samples from D2, H22 and 7-1 and was performed after creep rupture. D2 is 21.4° away from the 001 axis, a slightly lower strength orientation, and H22 is almost a sample of the -111 axis. 7-1 was selected for structural study after high temperature (982°C) deformation, which is believed to be a orientation which possesses nearly the same structure as any other bearing since there is no orientation dependency at this temperature. Figures 5-(a) through (c) are TEM microstructures of thin films which were sliced vertically on the tensile axis, near the rupture areas of D2, H22 and 7-1. In spite of the fact that D2 and H22 have been highly warped, their gamma' phases have

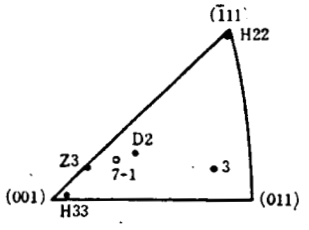

Fig. 4 Tensile axis orientation of samples used for metallography

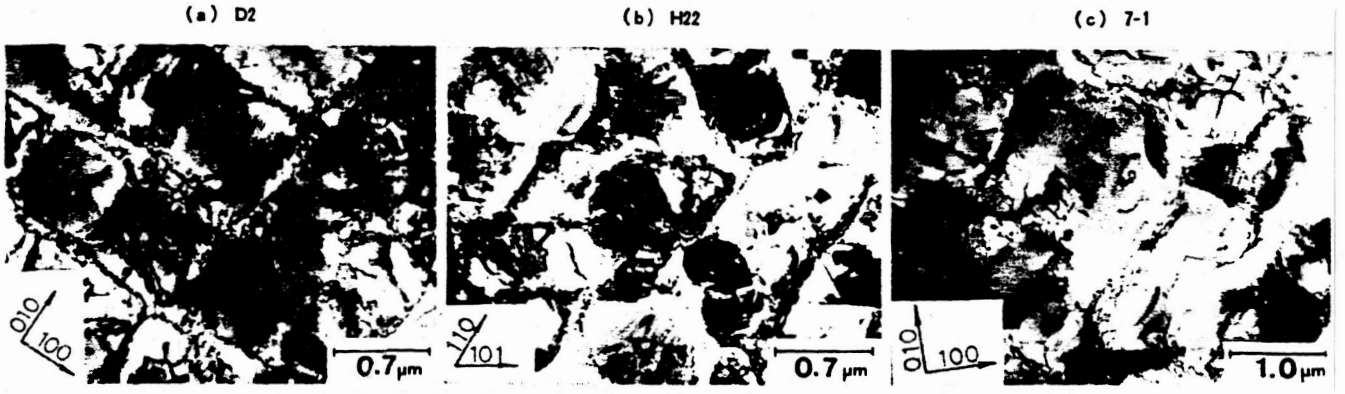

(note) thin films are perpendicular to tensile axes

Fig. 5 TEM microstructure at near rupture area of samples

retained their cubical geometric shape and arrangement. Contrasts in partial extended dislocation can be found in the gamma' phase, the dislocation activity being concentrated in the gamma phase, located in the spaces between gamma' phases and on the gamma-gamma' surfaces. /7

On the other hand, the regular arrangement and form of the gamma' phase of 7-1 is entirely disintegrated, and it can be seen that gamma' phase itself has received severe deformation and roughening during group deformation. Figure 6 shows the dislocation networks formed on the gamma-gamma' surfaces in 7-1, showing that dislocation reaction and rearrangement are promoted in the high temperature plastic flow of the gamma' phase.

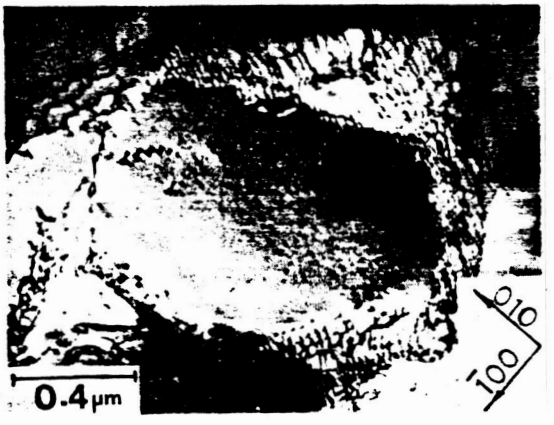

Fig. 6 γ-γ' interfacial dislocation net works formed in sample 7-1 crept at 982°C

4. Considerations

4.1 Temperature Dependency

When the data on samples which possess a tensile axis near the 001 axis is compared, σ_y and σ_B increase rapidly up to 700 to 800°C and decrease on the higher temperature side, showing behavior very similar to the characteristics of common cubic and columnar As explained above, in superalloys in which the gamma' content is near 60%, peculiarities in the deformation of the gamma' phase have a great deal of influence on the strength of that superalloy. The plastic deformation of the gamma' phase also shows maximum values in conjunction with high temperatures, these maximum values being where the {111} slip seen in common fcc alloys develops, but these maximum values displayed a great resistance to the action of angle dislocation by unexpectedly temporarily immobilizing this slippage [9]. It is believed that softening, after reaching maximum value is a response to the development of {100} slip, a peculiarity of L 1_2 standard phase, but there are few reports of clearly recognizable {100} slip in superalloy-type gamma-gamma' phase mixture alloys [10]. On the other hand, when the deformation temperature exceeds 900°C, many slip systems become active and it becomes a diffusion-penetrating plastic deformation and the gamma' phase experiences marked deformation and roughening under stress and dislocation. Increased dislocation action is also easily promoted through hole hyperactivity. Therefore, since the resistive effects to dislocation activity are minimal due to precipitates and the loss of isotropy, which is rooted in the slip plane and direction of

slippage, the strength of the superalloy is decided on the extent of precipitation hardening of the gamma phase or gamma' phase. As shown in Figure 1, Alloy 454 possesses a greater creep longevity, particularly on the high temperature side, when compared to the reference alloys, which is due largely either to the precipitation hardening of the gamma' phase through a high tantalum content, or to the structural uniformity due to the increased solution treatment temperature, and when considered from the aspect of application in turbine vanes, this bears great significance as concerns its application toward the improvement of strength at over 900°C.

4.2 Factors in the Determination of Orientation Dependency

The anisotropy of σ_y, creep rate and rupture longevity is clearly apparent at 760°C. This is thought to originate in temperature dependency, due to the belief that slip planes and slippage direction in dislocation are bound by crystallographic orientation. fcc structure metals commonly experience plastic deformation in a {111}<110> slip system, but in the Mar-M 200 [2]-[6] alloy referred to in this report, a {111}<112> system is activated in primary creep at 760°C, which is promoted by the shearing of gamma' areas by groups of extended partial dislocation, and as this progresses to secondary creep, the {111}<211> slip system cross-slips, developing full deformation hardening, afterwhich, its development is recognizable. Meanwhile, it has been observed in both stages of 875°C creeping, that twin a/2<110> dislocations are promoted through the shearing

of the gamma' phase. In L 1_2 standard phase, anti-phase boundaries (APB) are formed through the migration of twin a/2<110> dislocations, and these APB are eliminated by dislocations which possess Burgers vectors ($\vec{b}$) which are similar to the following, but since the energy of the {100} APB's is as much as one-tenth lower than that of {111}, {100} slip becomes more active at high temperatures. The Schmid Factor = $\cos\phi \times \cos\lambda$ which determines the shear stress as the angle of incidence (ϕ) and slip direction of the slip plane and the angle of incidence (λ) tensile axis, can be used to determine which slip system will be activated. The Schmid factor contours of the {111}<211>, 111 plane -101 axis and 001 plane -110 axis slip systems, showing the maximum shear stress load which they can bear, are shown in standard stereographic triangles in Figures 7-(a) through (c) for reference purposes. The maximum stress systems of the

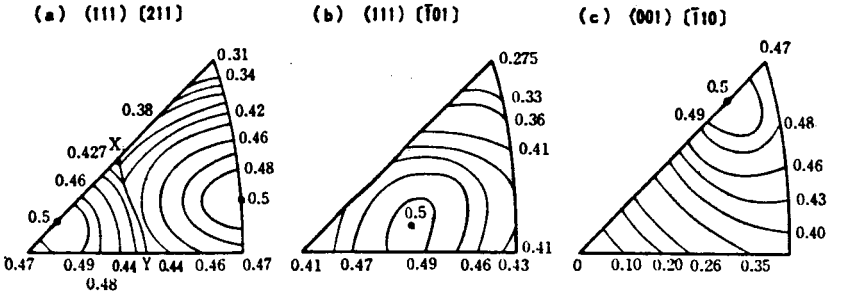

Fig. 7 Schmid factor contours for most highly stressed slip system

{111}<211> slip system are divided into -111 plane 11-2 axis and 111 plane 2-11 axis as the X-Y boundaries within the triangle. The tensile axis rotates to the slippage direction as the slip deformation advances, but since, theoretically, other slip

systems could also naturally reach maximum shear stress conditions and activate within the boundaries of the triangle, dislocation cross-slip could occur, work harden and initiate secondary creep. It is well known that because of this, the amount of time required until multiple slips have been initiated is determined by the relationship between the triangle boundaries and the starting position of the tensile axis and has a great deal of influence on the rate and longevity of subsequent creeping [5]. Another element which complicates the creep deformation behavior of nickel-based superalloys is the geometric arrangement of the gamma' phase. Since the cubic axes of the cubic gamma' phase are aligned right along the 100 family of axes, gamma phase spaces, which develop slippage relatively easily, exist among the crystals, between the gamma' phase. It is also understood that the relation between the orientation of the tensile axes and these spaces is also an important factor in easily determining slip systems.

4.3 Anisotropy of Alloy 454 (760°C) /8

Creep strength, σ_y is at maximum near the 001 axis, as compared to other orientations, with little change at tensile axes within 20° off-axis from the 001 axis. Figure 8 is the dislocation structure of a thin film sliced parallel to the 111

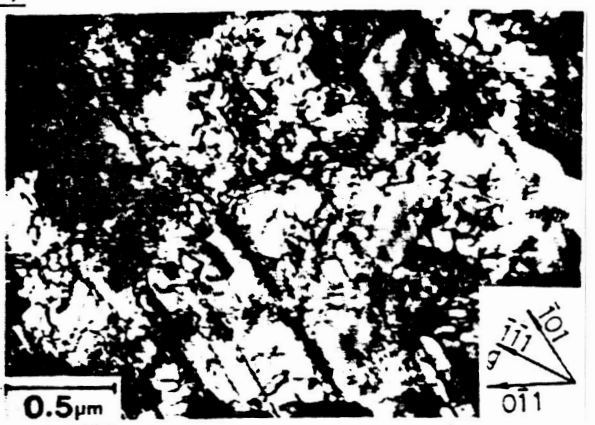

(note) thin film is nearly parallel to 111 plane

Fig. 8 Dislocation structure of sample H33

plane, which is the main slip plane of sample H22 (2° off-axis from the 001 axis), wherein dislocation groups which are nearly parallel to the -101 or 0-11 axes are visible, as well as in other planes within {111}, and a dislocation reaction has been started through cross-slip. Regions of high dislocation density are the spaces between gamma' phases and since gamma' phase cuboids are naturally arranged in a lattice-form, these regions are formed into nearly perpendicular bands. Meanwhile, several extended dislocation contrasts were observed among the gamma' phases in observation from the direction of the 001 axis, and it was established that each phase had nearly independently deformation hardened, allowing the substance resistance to creep deformation. As seen also in the Schmid factor mapping (Figure 7), {111}<110> and {111}<112> slip is relatively easy, but from the areas near the boundaries of the triangles, it is believed that multiple slip develops from fairly early in the creep stage. Creep strength is low in other alloys, particularly along the tensile axes which are nearly aligned with the 001 to -111 axis boundary. This is explained as originating in the high Schmid factor of the {111}<112> system, but it is believed that there is no decrease in the strength of this alloy since the degree of precipitation hardening of the gamma' phase is high compared to the that of the gamma phase in this alloy, making {111}<112> slip not so easy.

Reduction in creep strength near the 011 axis is believed to originate in the development and concentration of individual slips in the 111 plane -211 axis, according to conventional

explanations. Namely, another slip system does not need to be activated and harden since the tensile axis in sample 3 rotates an orientation relatively close to the maximum Schmid factor values for this slip system, while rotating in the direction of the -211 axis, namely, the direction of the 001 to -111 boundary line. This is clear from the condition of the slip axis observed in the vertical fracture plane of sample 3 after its deformation (Figure 12), and it was verified that this was the 111 plane from the thin film sample sliced parallel to the slip axis. The TEM dislocation structure of this sample is shown in Figure 9, but the noticeable difference from the 001 axis are the extended dislocations which penetrate extending through the gamma' cuboids in this sample, and it is believed that the <112> slip in these cuboids has developed throughout the entire sample in spite of the strength and orientation of the gamma prime phases, resembling the creep deformation mechanism at orientations relatively near the 001 axis in the Mar-M 200 alloy.

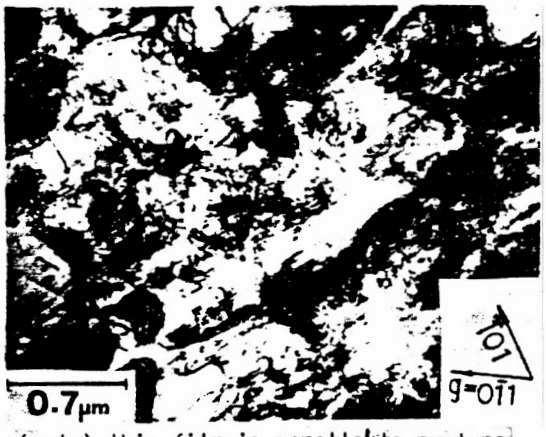

Fig. 9 Dislocation structure of sample 3

Creep strength near the -111 axis is nearly the same as data from the 011 axis orientation, which is markedly lower than data from this orientation in other alloys. The Schmid factors for {111}<112> and {111}<110> orientations, which are usually maximum strength orientations in other alloys, are minimal in this alloy,

which is explained by the fact that multiple cross-slip is easily developed in this alloy. Judging from these Schmid factors, 001 plane -110 axis slip would be easily developed, but there are no clear test facts which would indicate that what is observed in gamma' single-phase alloys will necessarily exist in gamma-gamma' two-phase alloys.

Nemoto, et al. report, through the TEM observation of the slip axes of single crystals near the -111 axis in high temperature (800°C) compression test samples of Rene' 80, that dislocation resultant from the geometric arrangement of the gamma' phases will concentratedly move the {100} between the gamma' phases as though a {001} slip had developed [11]. {111} slip bands of dislocation which cut through gamma' phases which are aligned nearly parallel with the 110 family of axes have also been observed in Rene' 80, but the volumetric content of gamma' phase in this alloy is nearly 10% higher than that of Rene' 80 (in other words, the gaps between the gamma' phases are narrower), helping to maintain the geometric arrangement even after fracture or rupture, as can be seen in Figure 5-(b). Figure 10 shows a structure observed from the position of plane 011, delineated 35° from the -111 tensile axis, in sample H22, but a group of dislocations exists on the 100 plane, which is between the gamma' phases

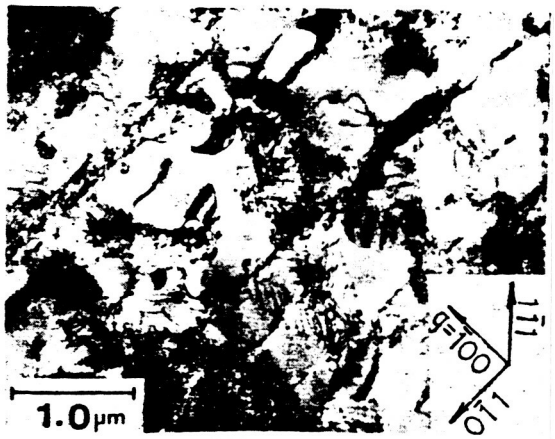

(note) thin film is nearly parallel to 011 plane

Fig. 10 Dislocation structure of sample H22

and perpendicular to the sample surface, which is parallel to the 01-1 axis. /9

Meanwhile, partially expanded dislocation exists at a shallower inclination, not in the gamma' phases, but only on the surfaces between the gamma and gamma' phases, while the extended dislocation contrast inside the gamma' phases is low. The results of observations of a 110 plane thin film sliced parallel to the tensile axis of a portion of low deformation separated from the fracture surface of the same sample in order to establish the Burgers vector of the structured dislocation are shown in Figures 11-(a)-(c). These figures ((a)-(c)) show the same region, which is parallel to the -111 tensile axis,

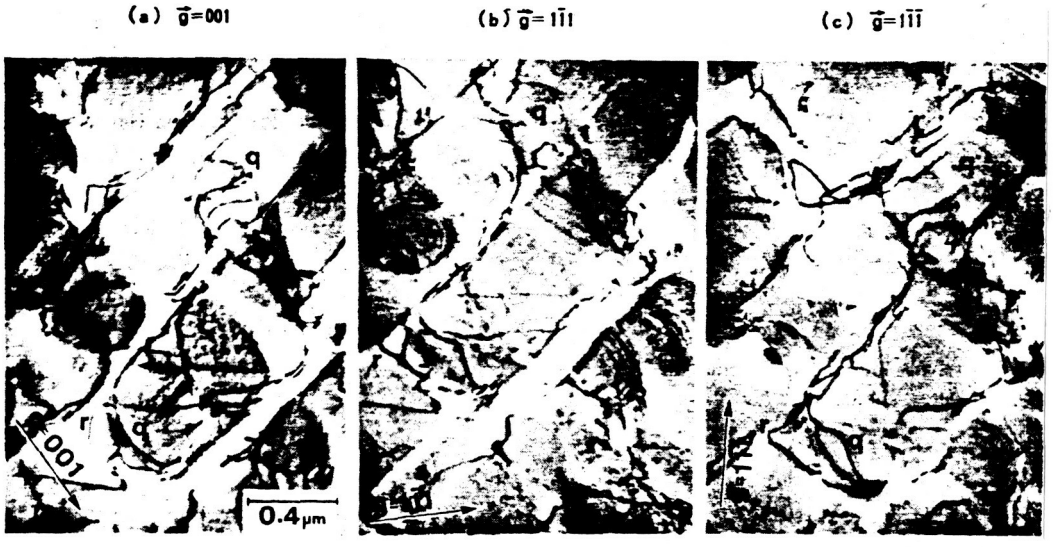

Fig. 11 Dislocation structure of sample H22 under different $\vec{g}$ vectors

observed under various reflection vectors, $\vec{g}$ = 001, 1-11, 1-1-1, and show that there is little extended dislocation contrast under any of the $\vec{g}$ vectors. From the evaluation of the

6 possible types of visible $\vec{b}$ = <110> and $\vec{g} \times \vec{b}$ dislocation contrasts (contrast disappears when $\vec{g} \times \vec{b} = 0$), it is understood that the $\vec{b}$ of the dislocation (q) is on the axis -101, and is believed to exist in addition to the dislocation (r) whose $\vec{b}$ is on the -110 axis of the 101 plane, parallel to the 001 plane. All of these combinations indicate the intense activity of the {100}<110> slip system. However, since dislocation (s) possessing $\vec{b}$ = -101 axis exists within the dislocation which is aligned nearly parallel to the 001 plane and will not allow slip on the 100 plane, it can be assumed that this slip is in the 111 family of planes. An alloy which reports this kind of low creep strength along the -111 axis orientation is only Ni-5 Al-2 Ti-9 Cr-12 W (PWA 1444)[10], which is the alloy in this testing, and creep strength along the -111 axis can be strengthened also in this alloy by adding 6% Re, a reinforcing element. Namely, the behavior of the -111 axis is largely related with the relative high temperature strengths of the gamma and gamma' phases and therefore, {100} slip and false {100} slip systems develop in alloys such as Alloy 454 and PWA 1444 since the shearing stress on the 100 family of planes between the gamma' phases is great when the strength of the gamma' phase is extremely high, as it is in these alloys. It is believed that since the gamma phase itself is also precipitation hardened in other alloys, the alloys are able to resist creep at the same time that shearing is advancing through the the {111}<211> slip system.

4.4 Rupture Forms

As a side note to the above explanation of anisotropy, post-testing photographs of the rupture surfaces of the samples Z 3, 3 and H22, which are near the 001, 011 and -111 tensile axes, viewed in cross section and parallel to the tensile axes, are shown in Figure 12. In contrast to the rough rupture in sample Z 3 which is nearly perpendicular to the tensile axis, the rupture surface of sample 3 is extremely smooth and determined, from X-rays, to be close to the 111 plane cleavage. Meanwhile, H22 has a roughly 45° rupture shape which is not smooth and possesses a rupture surface which is nearly parallel to the 100 family of planes, or namely, parallel to the primary dendrite growth direction, suggesting here also that dislocation slip is active.

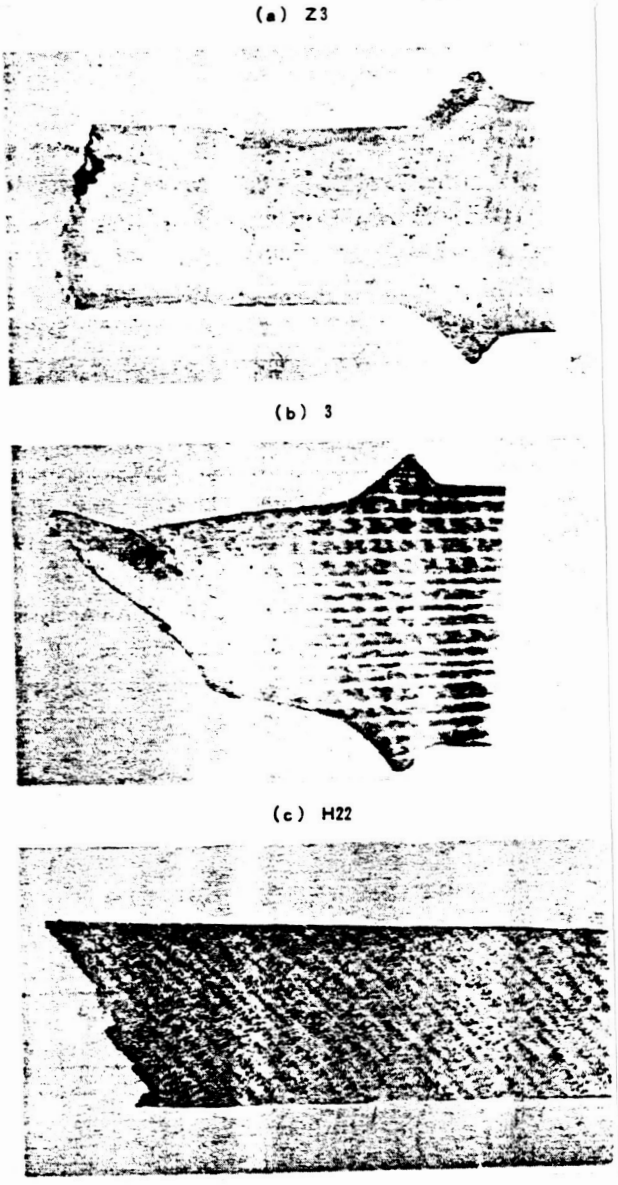

Fig. 12 Ruptured surface orientation of samples

5. Conclusion

/10

Anisotropy of the high temperature strength of Alloy 454 single crystals is marked at 760°C, at which point the gamma'

phase strength is at its peak, with orientations near the -111 and 011 tensile axes being extremely weak, those near the 001 axis being extremely strong and with practically no change in those within 20° off-axis from the 001 axis. Orientation dependency, determined from the distribution of creep rate and fracture longevity, can be classified schematically as in Figure 13. The following can be assumed about the mechanism of anisotropy through considerations drawn from Schmid factors and the TEM observation of dislocation microstructures.

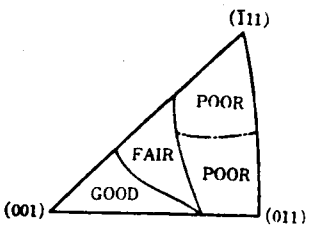

(note)the vicinities of planes 011 and -111 are each low in strength, but their deformation systems are different

Fig. 13 Schematic streographic triangle presentation of creep strength for Alloy 454 at about 760°C

1. When there is a tensile axis near the 001 axis, {111}<110> and {111}<112> slips will cause multiple slip in the gamma and gamma' phases and work hardening will start from the initial creep stage, providing excellent resistance to deformation.
2. When there is a tensile axis near the 011 axis, individual slip in the -211 axis of the 111 plane will mainly develop, cutting across the arrangement of the gamma' phases, resulting in a low degree of work hardening.
3. When there is a tensile axis near the -111 axis, shearing stress in the 100 family of planes between the gamma' phases is at its maximum and {100} and false {100} slip develops concentratedly in the gamma phase,

decreasing work hardening due to shearing in the gamma phase.

4. The reason that the strength of the -111 axis is particularly low compared to other alloys is believed to be due to the high tantalum content, used to reinforce the gamma' phase, of this alloy.

REFERENCES

(1) M. Gell, D.N. Duhl, A.F. Giamei: The Development of Single Crystal Superalloy Turbine Blades, Proc. of 4th International Conference "Superalloy 80", Sevensprings (1980, 9), pp. 205-214.

(2) B.H. Kear, G.R. Leverant, J.M. Oblak: An Analysis of Creep Induced Intrinsic/Extrinsic Fault Pairs in a Precipitation Hardened Nickel-Base Alloy, Trans. ASM, Vol. 62 (1969) pp. 639-650.

(3) G.R. Leverant, B.H. Kear: The Mechanism of Creep in Gamma Prime Precipitation-Hardened Nickel-Base Alloys at Intermediate Temperatures, Met. Trans., Vol. 1 (1970), pp.491-498.

(4) G.R. Leverant, B.H. Kear, J.M. Oblak: Creep of Precipitation-Hardened Nickel-Base Alloy Single Crystals at High Temperatures, Met. Trans., Vol. 4 (1973), pp.355-362.

(5) R.A. Mackay, R.D. Maier: The Influence of Orientation on the Stress Rupture Properties of Nickel-Base Superalloy Single Crystals, Met. Trans., Vol. 13A, (1982), pp.1747-1754.

(6) P. Caron, T. Khan: Improvement of Creep Strength in a Nickel-Base Single-Crystal Superalloy by Heat Treatment, Met. Sci. & Eng., Vol. 61, (1983), pp. 173-184.

(7) U.S. Patent 4209348, (1980).

(8) G. Matsumura (translator), rev. N. Kōda: Karitei X-sen Kaiseki Yōron (Carty X-ray Diffraction Essentials), Chapter 8, Agune Co.

(9) Nemoto, Echigoya, Sudō: Gamma'-Ni_3 (Al, Ti) Tankesshō-chū

no Teni Undō no HVEM Kensatsu (HVEM Observation of Dislocation Activity in Gamma'-Ni_3 (Al, Ti) Single Crystals), Nihon Kinzoku Gakkaishi (Japanese Metals Society Magazine), Vol. 44, No. 8, August 1980, pp. 925-932.

(10) A.F Giamei: Deformation of Advanced Anisotropic Superalloys, Final Report for Air Force Office of Scientific Research, AFOSR-TR-80-0033 (November 1979).

(11) Nemoto, Honda, Echigoya, Sudō: Ni-ki Chōgōkin Rene' 80 no Kasei Henkeichū no Teni Kyodō (Dislocation Behavior during Plastic Deformation of Nickel-Based Superalloy Rene-80), Nihon Kinzoku Gakkaishi (Japanese Metals Society Magazine), Vol. 44, No. 8, August 1980, pp. 933-942.

ACKNOWLEDGMENTS

Part of this research is based on the System for the Research and Development of Basic Technology for Next Generation Industries of the Ministry of International Trade and Industries' Institute of Industrial Technology, and was performed as a part of the "Research and Development of High Performance Crystal Controlled Alloys" under the direction of, and with a grant from, the Society for the Research and Development of Next Generation Metals and Composite Materials. We would like to thank Professor Nemoto of Kyushu University and Mr. Harada of the Metal Materials Technical Research Laboratory for their indispensable assistance and advice.